PLANT SCIENCE TODAY
ISSN 2348-1900 (online)
Vol 11(4): 314-322
https://doi.org/10.14719/pst.3221

HORIZON
e-Publishing Group
HePG

RESEARCH ARTICLE

Green synthesis and antibacterial potency of Ag/CuO/ZnO nanoparticles derived from *Psidium guajava* L. extracts

Richa Bhardwaj[1], Devyani Naruka[1], Neha Kapoor[2] & Lokesh Gambhir[3]*

[1]Department of Botany, IIS (Deemed To Be University), Jaipur, Rajasthan-302 020, India
[2]School of Applied Sciences, Suresh GyanVihar University, Jaipur, Rajasthan-302 017, India
[3]School of Basic and Applied Sciences, Shri Guru Ram Rai University, Dehradun, Uttarakhand-248 001, India

*Email: gambhir.lokesh@gmail.com

OPEN ACCESS

ARTICLE HISTORY
Received: 25 December 2023
Accepted: 24 May 2024
Available online
Version 1.0 : 30 September 2024
Version 2.0 : 01 October 2024

Check for updates

Additional information

Peer review: Publisher thanks Sectional Editor and the other anonymous reviewers for their contribution to the peer review of this work.

Reprints & permissions information is available at https://horizonepublishing.com/journals/index.php/PST/open_access_policy

Publisher's Note: Horizon e-Publishing Group remains neutral with regard to jurisdictional claims in published maps and institutional affiliations.

Indexing: Plant Science Today, published by Horizon e-Publishing Group, is covered by Scopus, Web of Science, BIOSIS Previews, Clarivate Analytics, NAAS, UGC Care, etc
See https://horizonepublishing.com/journals/index.php/PST/indexing_abstracting

CITE THIS ARTICLE

Bhardwaj R, Naruka D, Kapoor N, Gambhir L. Green synthesis and antibacterial potency of Ag/CuO/ZnO nanoparticles derived from *Psidium guajava* L. extracts . Plant Science Today. 2024; 11(4): 314-322. https://doi.org/10.14719/pst.3221

Abstract

Nanoparticles, characterized by their unique physicochemical properties, represent a significant frontier in interdisciplinary research, particularly within the realms of biomedicine and environmental science. This investigation delves into the eco-friendly synthesis of silver (Ag), copper oxide (CuO) and zinc oxide (ZnO) nanoparticles utilizing extracts derived from *Psidium guajava* L. The utilization of these botanical extracts presents a sustainable alternative to traditional nanoparticle fabrication methodologies, aligning with global sustainability imperatives and fostering environmentally conscious practices. The escalating global nanoparticle market, valued at over $30 billion in 2020 and projected to surpass $90 billion by 2027, underscores the economic significance and industrial relevance of nanoparticle research. This research trajectory fuels innovation across a spectrum of sectors, including healthcare, cosmetics and environmental remediation. The commercialization of nanoparticle-based products not only drives substantial revenue streams but also catalyzes advancements in research, development and manufacturing endeavors. Drawing upon aqueous extracts sourced from *P. guajava*, leaves and fruits, this study capitalizes on their inherent phytochemical composition to serve as stabilizing, reducing and capping agents during nanoparticle synthesis. Employing state-of-the-art characterization techniques such as UV-Vis spectroscopy, FTIR spectroscopy, FE-SEM and EDS facilitates a comprehensive analysis of the synthesized nanoparticles' physicochemical attributes. Assessment of the nanoparticles' antibacterial efficacy against gram-positive (*Bacillus subtilis, Staphylococcus aureus*) and gram-negative (*Escherichia coli, Proteus vulgaris*) bacterial strains reveals compelling results. Minimum inhibitory concentrations (MIC) elucidate notable efficacy, notably against *P. vulgaris* (3.75 mg/mL), *S. aureus* (7.5 mg/mL) and *B. subtilis* (10 mg/mL and 12.5 mg/mL), indicative of their potential biomedical applications in combating microbial infections.

Keywords

Green nanoparticles; MIC; FESEM; ESD

Introduction

The burgeoning field of nanomaterials has garnered significant attention for their wide-ranging applications across various sectors (1). Nanoparticles, characterized by their minute size (1–100 nm) and unique properties including shape, surface reactivity and charge, offer versatile functionalities. However, traditional chemical-based nanoparticle synthesis, often involving

heavy metals, poses environmental risks due to the release of toxic by-products. In response, green nanoparticle synthesis methods utilizing natural bioactive components as reducing, capping and stabilizing agents have emerged as environmentally friendly alternatives (2). Plant extracts derived from leaves, fruits, bark and roots serve as effective reducing and stabilizing agents in green nanoparticle synthesis (3). Numerous studies have demonstrated the pharmaceutical potential of green nanoparticles synthesized from various plant extracts, including *Calotropis gigantea, Syzygium cumini, Ziziphus spina-christi* and *Azadirachta indica* (4, 5). These nanoparticles exhibit antibacterial, antifungal, antiparasitic, antiviral and anticancer activities (6, 7). In addition to plant extracts, charred biowaste presents an innovative and sustainable feedstock for the synthesis of carbon-based nanoparticles, further enhancing the eco-friendliness of nanoparticle production processes. Charred biowaste, such as agricultural residues, wood chips and biochar, contains carbonaceous material that can be utilized as a precursor for carbon nanoparticles (8). The utilization of charred biowaste as a feedstock for nanoparticle synthesis offers several advantages, as it promotes the efficient utilization of agricultural residues and biomass, thereby reducing waste and contributing to sustainable waste management practices (9). Secondly, charred biowaste provides a renewable and abundant source of carbon, mitigating the need for synthetic carbon precursors derived from fossil fuels (10). Nanoparticles are driving innovation in the energy industry, offering solutions for clean energy generation, efficient energy storage, catalytic processes, lighting technologies, thermal management, oil and gas exploration and nuclear energy applications (11). Green nanoparticles using Fe, Cu, Ni, Ag, Au and Ti have been reported to enhance biohydrogen production via various biological pathways to meet global energy demand (12). Many such nanoparticles, specifically those derived from metals such as silver (Ag), gold (Au), copper (Cu), zinc (Zn), iron (Fe) and graphene have shown potent antimicrobial and therapeutic properties (13-15). Plant extracts from species like *Eucalyptus globules, Lantana camara* and *Ginkgo biloba* have been utilized for the synthesis of Ag nanoparticles with notable antibacterial, antifungal and anticancer effects (16-18). Cu and CuO nanoparticles synthesized using plant leaf extracts of *Psidium guajava*, *E. globulus* and *C. gigantean* demonstrate degradation of organic pollutants, antibacterial, antifungal, photovoltaic and antioxidant properties (19-21). Similarly, Zn and ZnO nanoparticles synthesized from leaf extracts of *Moringa oleifera*, *Aloe barbadensis* and fruit extracts of *Citrus aurantifolia* and *Garcinia xanthochymus* exhibit antibacterial, antibiofilm and antioxidant activities (22). Given the rise of multidrug-resistant (MDR) bacteria, the search for novel antibacterial agents is imperative. Green nanoparticles synthesized from medicinal plants offer a promising avenue for combating MDR pathogens (23-26). *P. guajava*, a tropical plant with a rich history of medicinal use, serves as a valuable source for the synthesis of Ag, CuO, and ZnO nanoparticles with potential antibacterial activity against MDR strains (27). This study contributes to the exploration of natural resources for the development of effective antimicrobial agents and green nanoparticle synthesis from natural sources intersects environmental stewardship, economic prosperity, public health and technological advancement. Green nanoparticle synthesis methods offer economic benefits through cost savings, revenue generation and market competitiveness. By addressing environmental challenges while unlocking economic opportunities, this research contributes to the transition toward a more sustainable and resilient future.

Materials and Methods

Synthesis of green nanoparticles

Fresh leaves and fruits were collected from Gangapur city, Rajasthan and identified at the Herbarium, Department of Botany, IIS (Deemed to be University), Jaipur. These plant materials were washed, shade-dried and ground to a fine powder. Extracts were prepared by mixing 10 g of dried leaf and fruit powder with 100 mL of distilled water, separately boiled at 90 °C and kept to cool at room temperature. Later, the mixture was centrifuged at 6000 rpm for 25 min. and the extract was filtered using Whatman filter paper. The extracts prepared were further used for nanoparticle synthesis.

Silver nanoparticles (AgNPs)

AgNPs were synthesized following the previously described protocols (28, 29). Briefly, 5 mL of extract was mixed with 1 mM aqueous $AgNO_3$ solution, stirred for 30 min. and kept overnight for reduction. AgNPs were separated by centrifugation at 10000 rpm for 30 min, washed thrice with deionized water and dried at 90 °C.

Copper oxide nanoparticles (CuONPs)

CuONPs were synthesized following the previously described protocols with some modifications (30, 31). Briefly, 10 mL of each extract was added dropwise to 100 mL of 5 mM $CuSO_4.5H_2O$, stirred with heating at 90 °C, color change was observed within 2 h. Prepared CuONPs were separated by centrifugation at 10000 rpm for 30 min, washed thrice with distilled water, and kept for drying at 90 °C.

Zinc oxide nanoparticles (ZnONPs)

ZnONPs were synthesized using a modified version of the protocol outlined (32). Initially, a 50 mL solution containing 10 % aqueous zinc acetate was prepared and subjected to stirring for 30 min. Subsequently, 10 mL of an extract was gradually added dropwise, after which the mixture was placed on a magnetic stirrer for 2 h under ambient conditions with the pH 12 maintained. The resulting solution was then allowed to incubate undisturbed for 12 h. The nanoparticles synthesized under alkaline conditions exhibited a transmission rate of 84 % within the visible and infrared spectra. The solution was centrifuged at 5000 rpm for 20 min after synthesis. The resultant residue was subjected to washing with 80 % ethanol, followed by 3 subsequent washes with distilled water. Finally, the washed precipitate was dried at 120 °C to yield the synthesized nanoparticles.

Characterization of synthesized green nanoparticles

The synthesized nanoparticles were rigorously characterized to ascertain their properties. The UV-Vis spectrophotometry (PerkinElmer, USA) was employed to determine their absorbance spectra within the wavelength range of 200 to 600 nm, facilitating the estimation of band gap energy. Additionally, the morphology, size, shape and dispersal tendencies of the nanoparticles were meticulously analyzed utilizing Field Emission Scanning Electron Microscopy (FE-SEM) (Carl Zeiss, Germany). Elemental composition was elucidated through Energy Dispersive X-ray Spectroscopy (EDX) (TESCAN USA) to confirm the presence of constituent elements. Further insight into the chemical composition was garnered via Fourier Transform Infrared (FTIR) spectroscopy (PerkinElmer, USA), which provided data on functional groups present in the nanoparticles, covering a wavenumber range from 500 to 4000 cm^{-1}.

Agar well diffusion assay

The antibacterial potential of the nanoparticles was assessed via the agar well diffusion method, with modifications implemented under sterile conditions (33). Four bacterial strains—*Bacillus subtilis* (MTCC-441), *Staphylococcus aureus* (MTCC-737), *Escherichia coli* (MTCC-739) and *Proteus vulgaris* (MTCC-426)—served as test organisms. Standardized inoculum was prepared using a 0.5 McFarland solution. Following inoculation onto agar plates, incubation was carried out at 37 °C for 18 h. Antibacterial activity was determined by measuring inhibition zones around nanoparticle-loaded wells, with concentrations of 20 mg/mL and 50 mg/mL tested. Petri dishes were then incubated at 37 °C for 20–24 h. Data represents averages of 3 independent experiments. Furthermore, the minimum inhibitory concentration (MIC) of the synthesized nanoparticles, defined as the lowest nanoparticle concentration eliciting inhibition of bacterial growth, was assessed using the agar well diffusion method against the target pathogens. Wells were loaded with 30 µL of aqueous nanoparticle solutions at concentrations ranging from 20 to 1.75 mg/mL. After incubation at 37 °C for 18 h, MIC was determined.

Statistical analysis

The statistical analysis was carried out by employing Analysis of Variance (ANOVA) in GraphPad Prism 5 software, followed by post hoc analysis by Tukey's test ($p<0.05$). All the data is represented in triplicates and 3 independent experiments were performed for each test.

Results and Discussion

Biosynthesis of green nanoparticles

In this investigation, aqueous extracts derived from *Psidium guajava* leaves and fruits were employed as agents for the biosynthesis of green nanoparticles. Fig. 1 delineates the synthesis process: (A) showcases the generation of AgNPs, characterized initially by orange-brownish and pale yellowish hues, transitioning to blackish and brownish tones following a 20 h incubation period; (B) illustrates the formation of CuONPs, featuring initial orange-brownish and green-yellowish colorations, which subsequently transformed into blackish and green-brownish precipitates after 2 h of incubation. Lastly, (C) delineates the synthesis of ZnONPs, with initial yellow-brownish and pale yellowish precipitates evolving into brownish and white precipitates, respectively, over a 20 h incubation period. These alterations in coloration and the formation of precipitates signify the successful synthesis of nanoparticles.

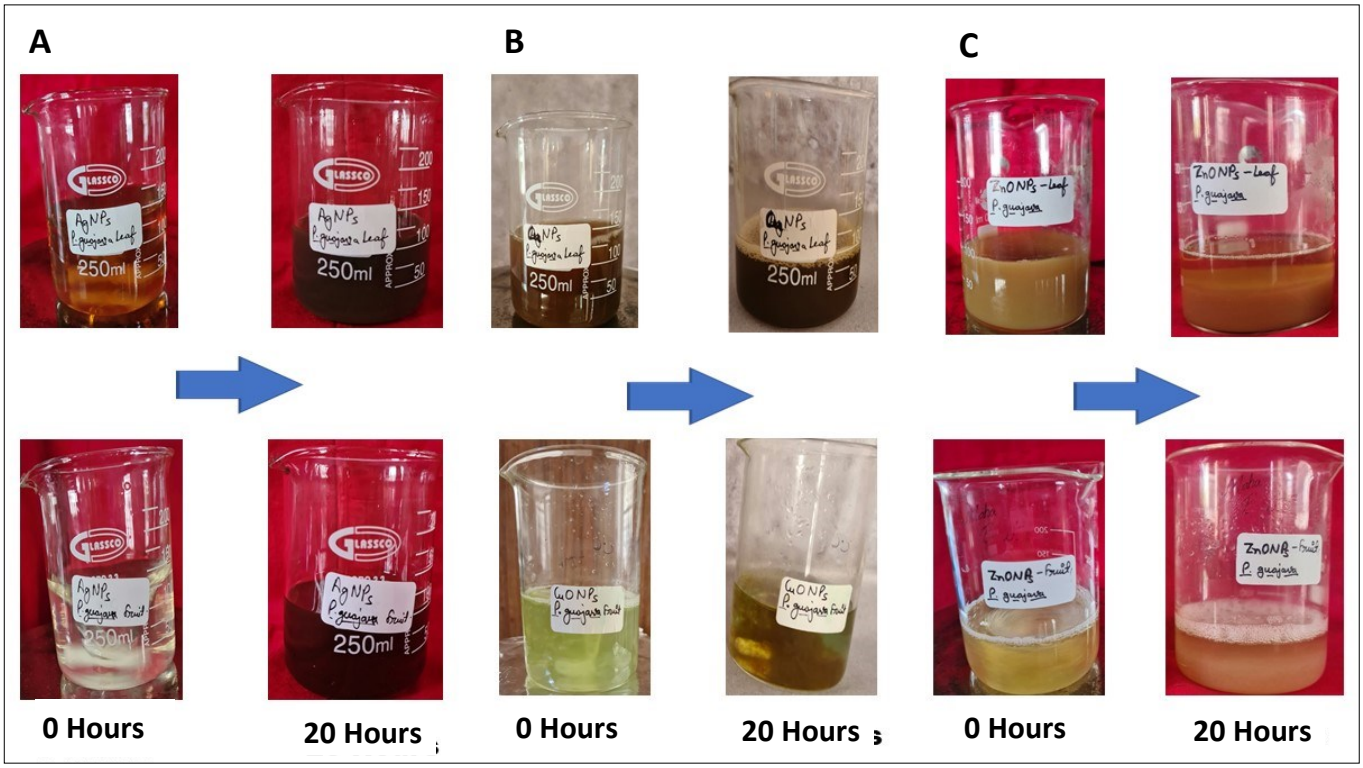

Fig. 1. Green synthesis of nanoparticles from leaf and fruit extracts: Change in colour results in the formation of nanoparticles (**A**) Synthesis of AgNPs (at 20 h.) (**B**) Synthesis of CuONPs (at 20 h.) (**C**) Synthesis of ZnONPs (at 24 h.).

UV-Vis spectroscopy analysis of synthesized green nanoparticles

Fig. 2 shows the UV-Vis spectroscopy results for the characterization of synthesized green nanoparticles in the range of 200–600 nm. In graphs, the graph (A) indicates the maximum absorption peaks at 412 nm for leaf-mediated AgNPs and at 420 nm for fruit-mediated AgNPs. The results attained were in coherence with another study, for the characterization of green synthesized AgNPs using *Capsicum annum* L. extract, exhibiting the maximum resonance at 420 nm (34). Graph (B) shows maximum peaks at 242 nm were observed for leaf-mediated CuONPs and for fruit-mediated CuONPs at 242 nm. The results were similar to the UV-Vis spectroscopy characterization of green nanoparticles synthesized using extracts of spices including star anise, mace and nutmeg (35). Graph (C) indicates the maximum peak observed for leaf-mediated ZnONPs at 241 nm and for fruit-mediated ZnONPs at 239 nm.

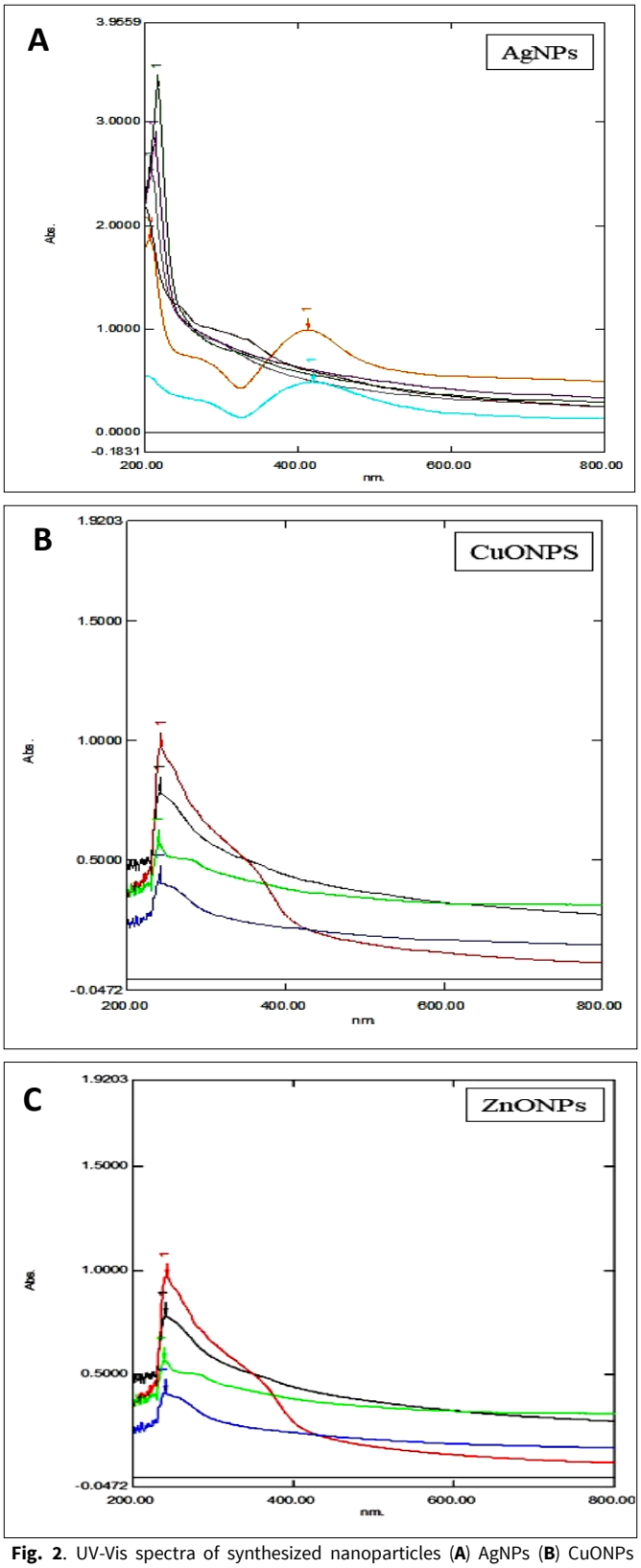

Fig. 2. UV-Vis spectra of synthesized nanoparticles (**A**) AgNPs (**B**) CuONPs (**C**) ZnONPs.

Analysis of synthesized nanoparticles using FTIR spectroscopy

The functional groups present in the synthesized nanoparticles were analyzed using Fourier Transform Infrared (FTIR) spectroscopy. Fig. 3 displays the FTIR spectra, with distinctive peaks indicating the presence of specific functional groups. In leaf-mediated AgNPs (spectra A), the observed broad bands at 3432.48 cm^{-1} correspond to OH groups, while peaks at 1263.78 cm^{-1} denote C-O stretching, 1028.68 cm^{-1} signify sulfoxides and 802.99 cm^{-1} represent C-H bending. For fruit-mediated AgNPs (spectra B), the broad band at 3431.13 cm^{-1} indicates -OH groups, with peaks at 1263.01 cm^{-1} suggesting C-O stretching, 1093.77 cm^{-1} representing anhydrides, 1025.01 cm^{-1} indicating sulfox-

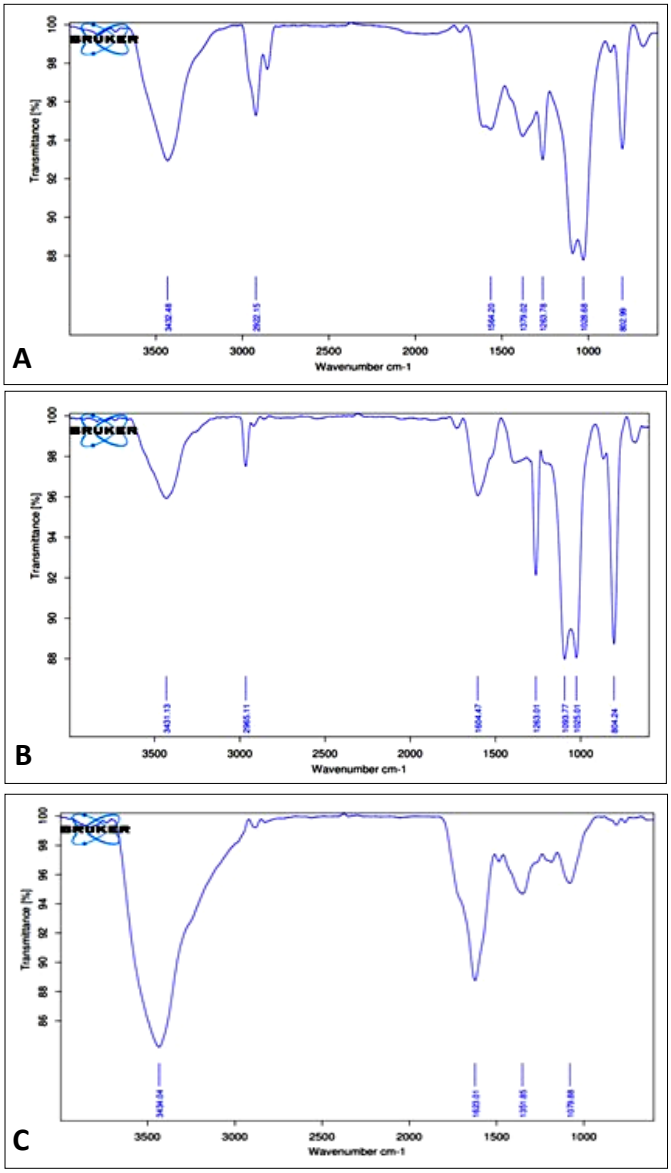

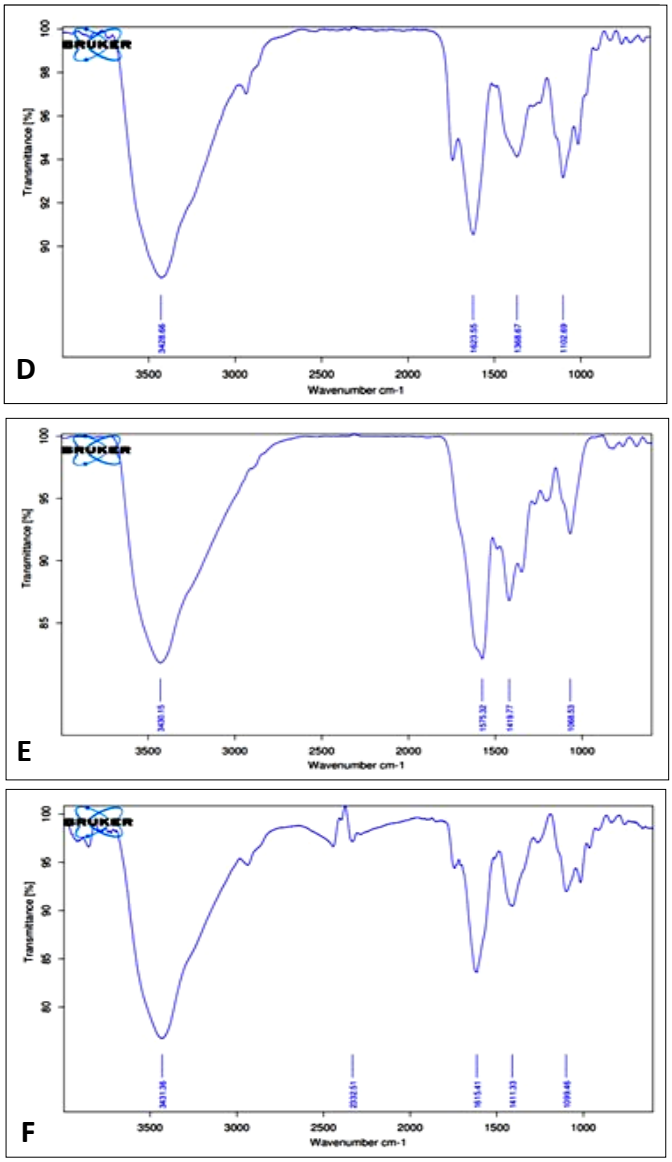

Fig. 3. FTIR of synthesized nanoparticles (**A**) AgNPs-Leaf (**B**) AgNPs-Fruit (**C**) CuONPs-Leaf (**D**) CuONPs-Fruit (**E**) ZnONPs-Leaf (**F**) ZnONPs-Fruit .

ides and 804.24 cm^{-1} representing C-H bending. In leaf-mediated CuONPs (spectra C), the broadband at 3434.04 cm^{-1} signifies -OH groups, while peaks at 1623.01 cm^{-1} denote aromatic compounds, 1351.85 cm^{-1} suggest alkanes and 1079.88 cm^{-1} indicate anhydrides. For fruit-mediated CuONPs (spectra D), the broad band at 3428.66 cm^{-1} indicates -OH groups, with peaks at 1623.55 cm^{-1} suggesting alkanes, 1368.67 cm^{-1} indicating phenols and 1102.69 cm^{-1} denoting fluoro compounds. Additionally, peaks at 624 cm^{-1}, 701 cm^{-1} and 777 cm^{-1} are attributed to the biosynthesis of CuO, while peaks at 799 cm^{-1} and 855 cm^{-1} represent the vibration modes of CuONPs (36). In leaf-mediated ZnONPs (spectra E), the broad band at 3430.15 cm^{-1} signifies -OH groups, while peaks at 1575.32 cm^{-1} represent nitro compounds, 1419.77 cm^{-1} denote alcohols and 1068.53 cm^{-1} indicate sulfoxides. For fruit-mediated ZnONPs (spectra F), the broadband at 3431.36 cm^{-1} indicates -OH groups, with peaks at 1615.41 cm^{-1} suggesting unsaturated ketones, 1411.33 cm^{-1} indicating sulfonyl chlorides and 1099.46 cm^{-1} representing secondary alcohols. These observed spectral features closely align with another report (32).

Analysis of green nanoparticles using FESEM and EDS

The Field Emission Scanning Electron Microscopy (FESEM) technique was employed to analyze the size and morphology of the synthesized nanoparticles, while Energy Dispersive X-ray Spectroscopy (EDS), integrated with FESEM, facilitated the determination of elemental composition. Fig. 4 illustrates the FESEM images of AgNPs synthesized using leaf (A) and fruit extract (B) of *P. guajava*, revealing smooth spherical shapes with a size distribution ranging from 20 to 41 nm. EDS analysis depicted peaks corresponding to high concentrations of Ag, along with lower concentrations of Cl, C and O. These findings align with the previous study (37). Furthermore, Fig. 5 displays the FESEM and EDS results for synthesized CuONPs. Leaf extract-mediated CuONPs (A) exhibited asymmetrical-spherical shapes with sizes ranging from 15 to 40 nm, while fruit extract-mediated CuONPs (B) appeared as asymmetrical-cuboidal shapes with sizes ranging from 50 to 107 nm. EDS analysis revealed the presence of high concentrations of Cu, along with traces of C, Ca, Cl and O, consistent with the previously reported observations (38). Lastly, Fig. 6 depicts FESEM images of ZnONPs synthesized using leaf and fruit extract of *P. guajava* (A and B), showcasing asymmetrical shapes with size ranges from 20–90 nm. EDS analysis indicated high concentrations of Zn, accompanied by low concentrations of C and O, consistent with previous reports utilizing *Cayratia pedata* and *P. guajava* leaf extract (39).

Analysis of antibacterial potential of green nanoparticles

The antibacterial efficacy of nanoparticles synthesized via green methodologies was systematically evaluated against a spectrum of bacterial strains, including *Bacillus subtilis*, *Staphylococcus aureus*, *Escherichia coli* and *Proteus vulgaris*. Each nanoparticle variant was evaluated at concentrations of 20 mg/mL and 50 mg/mL, employing the agar well diffusion method. AgNPs produced with aqueous leaf extract of *P. guajava* exhibited notable antibacterial activity, with prominent effects observed at 20 mg/mL against *P. vulgaris* (zone of inhibition [ZOI]: 10.33 ± 1.25 mm) and at 50 mg/mL against *B. subtilis* (ZOI: 17.66 ± 1.25 mm). Conversely, AgNPs synthesized with fruit extract demonstrated heightened activity at 20 mg/mL against *S. aureus* (ZOI: 12 ± 0.82 mm) and at 50 mg/mL against *E. coli* (ZOI: 10.33 ± 2.05 mm). CuONPs prepared with leaf extract manifested significant antibacterial effects, notably evident at 20 mg/mL against *P. vulgaris* (ZOI: 21 ± 1.63 mm) and at 50 mg/mL against *B. subtilis* (ZOI: 23.33 ± 1.25 mm). Similarly, CuONPs synthesized with fruit extract displayed considerable activity, notably at 20 mg/mL against *B. subtilis* (ZOI: 22 ± 2.45 mm) and at 50 mg/mL against *B. subtilis* (ZOI: 25 ± 3.74 mm). ZnONPs generated with leaf extract showcased noteworthy antibacterial properties, particularly discernible at 20 mg/mL against *B. subtilis* (ZOI: 19 ± 1.63 mm) and at 50 mg/mL against *B. subtilis* (ZOI: 23.33 ± 1.7 mm). Similarly, ZnONPs synthesized with fruit extract exhibited substantial activity, particularly at 20 mg/mL against *B. subtilis* (ZOI: 18.33 ± 1.25 mm) and at 50 mg/mL against *B. subtilis* (ZOI: 22 ± 2.16 mm) (Fig. 7). Furthermore, the Minimum Inhibitory Concentration (MIC) of the synthesized nanoparticles was determined. These MIC

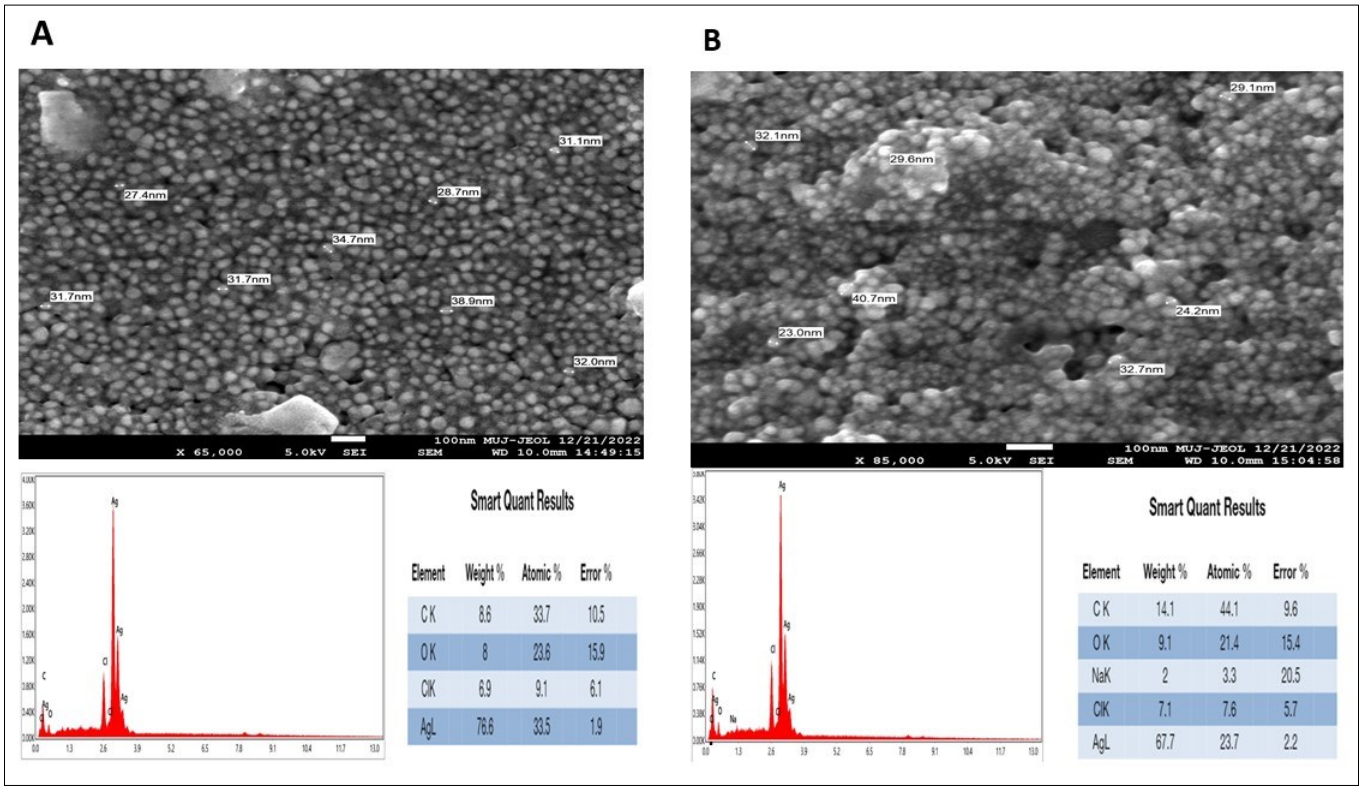

Fig. 4. Characterization of synthesized nanoparticles: FESEM and EDS of AgNPs (**A**) Leaf (**B**) Fruit revealing smooth spherical shapes with a size distribution ranging from 20 to 41 nm. EDS analysis depicted peaks corresponding to high concentrations of Ag, along with lower concentrations of Cl, C and O.

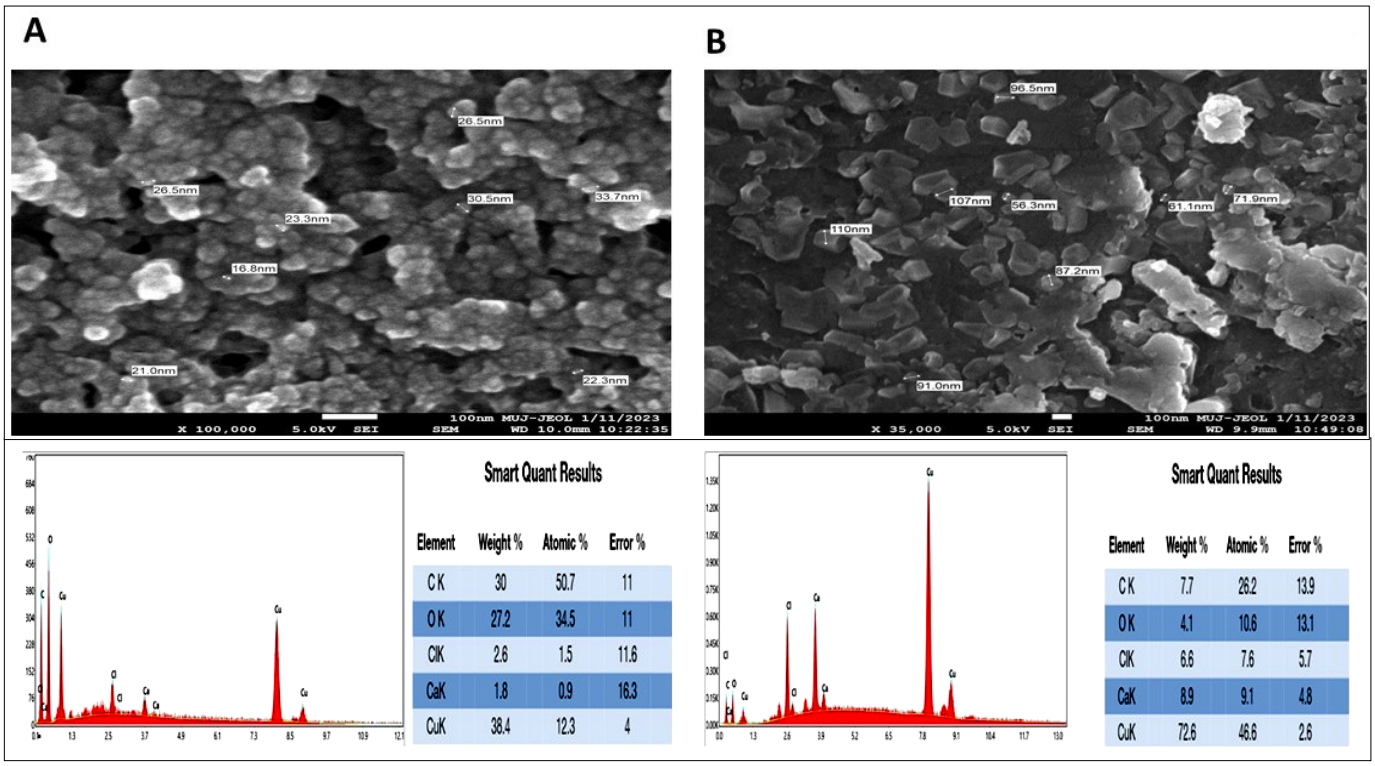

Fig. 5. Characterization of synthesized nanoparticles: FESEM and EDS of CuONPs (**A**) Leaf: (**B**) Fruit Leaf extract-mediated CuONPs (A) exhibited asymmetrical-spherical shapes with sizes ranging from 15 to 40 nm, while fruit extract-mediated CuONPs (B) appeared as asymmetrical-cuboidal shapes with sizes ranging from 50 to 107 nm. EDS analysis revealed the presence of high concentrations of Cu, along with traces of C, Ca, Cl and O.

values offered insights into their potency against specific bacterial strains. Leaf-mediated AgNPs displayed MIC against *P. vulgaris* at 3.75 mg/mL, while fruit-mediated AgNPs demonstrated MIC against *S. aureus* at 7.5 mg/mL. Leaf-mediated CuONPs exhibited MIC against *B. subtilis*, *S. aureus* and *P. vulgaris* at 3.75 mg/mL and fruit-mediated CuONPs exhibited MIC against *B. subtilis* at 7.5 mg/mL. Leaf-mediated ZnONPs demonstrated MIC against *B. subtilis* at 10 mg/mL, whereas fruit-mediated ZnONPs exhibited MIC against *B. subtilis* at 12.5 mg/mL (Table 1). The study thus conducted confirms the proper synthesis of green nanoparticles. The proposed research represents an industrially promising approach to combat antibiotic resistance and advancing sustainable nanotechnology. By leveraging the rich biodiversity of natural plant-based materials, this concept aims to contribute to the development of innovative solutions with broad applications in healthcare and antibiotic production.

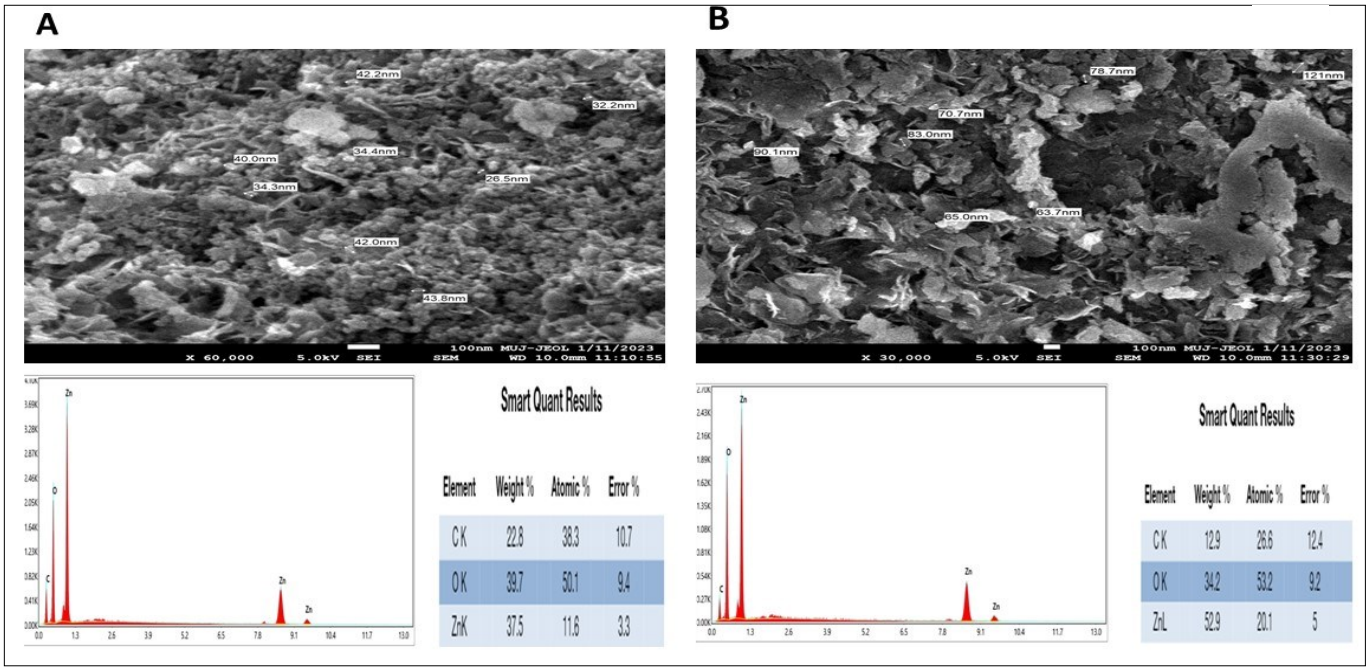

Fig. 6. Characterization of synthesized nanoparticles: FESEM and EDS of ZnONPs (**A**) Leaf (**B**) Fruit showcasing asymmetrical shapes with size ranges of 20–90 nm. EDS analysis indicated high concentrations of Zn, accompanied by low concentrations of C and O.

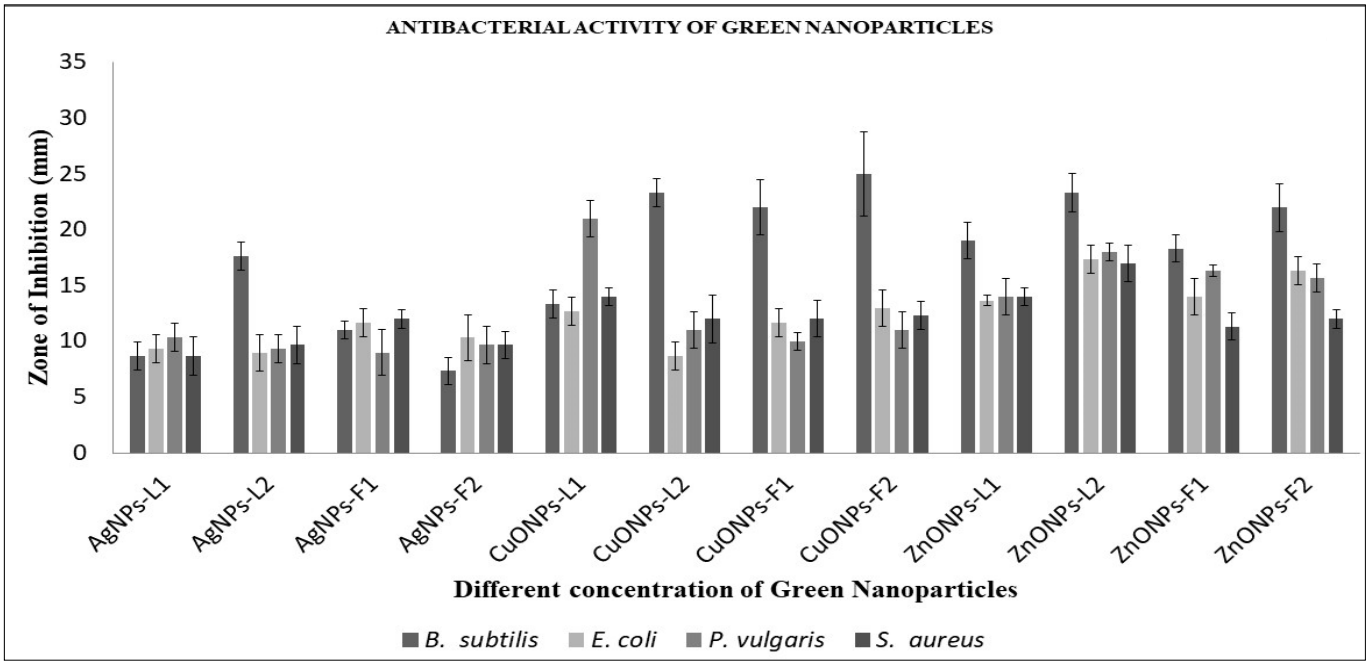

Fig. 7. *In vitro* antibacterial activity of different concentrations of green nanoparticles against *S. aureus, E. coli, P. vulgaris,* and *B. subtilis*. CuONPs from fruit extracts at conc. 50 mg/mL was observed to exhibit prominent antibacterial activity against *B. subtilis* followed by leaf extracts based CuONPs and ZnONPs at 50 mg/mL as per One Way ANOVA analysis [F{12,24)=22.17, p<0.0001] and Tukey's post hoc analysis. In case of *S. aureus* and *E.coli*, ZnONPs from leaf extracts at 50 mg/mL exhibited notable antibacterial activity as per One way ANOVA with F(12,24)=5.241 and 7.906 respectively at p<0.0001 and Tukey's Post hoc analysis. CuONPs from leaf extracts at 20 mg/mL exhibited substantial antibacterial activity against *P. vulgaris* followed by leaf extract based ZnoNPs at 20 mg/mL as per one way ANOVA [F(12,24)=14.39, p<0.0001] and Tukey's Post hoc analysis. The inhibition zones (in mm) are represented as Mean ± SD of three replicates. Means represented with different letters as well as color codes are significantly different by Tukey's Post Hoc Test at p<0.05**.**

Table 1. Minimum inhibitory concentration (mg/mL) of the synthesized NPs.

Test Pathogen	Nanoparticle concentration (mg/mL)					
	AgNP-Leaf	AgNP-Fruit	CuONP-Leaf	CuONP-Fruit	ZnONP-Leaf	ZnONP-Fruit
Bacillus subtilis	7.5 ± 0.5^{b}	10 ± 0.0^{c}	3.75 ± 0.25^{a}	7.5 ± 0.5^{b}	10 ± 0.5^{c}	12.5 ± 0.5^{d}
Escherichia coli	7.5 ± 0.6^{a}	12.5 ± 0.5^{b}	7.5 ± 0.5^{a}	12.5 ± 0.5^{b}	12.5 ± 0.5^{b}	15 ± 0.3^{c}
Proteus vulgaris	3.75 ± 0.25^{a}	10 ± 0.5^{b}	3.75 ± 0.25^{a}	10 ± 0.5^{b}	15 ± 0.5^{c}	17.5 ± 0.5^{d}
Staphylococcus aureus	7.5 ± 0.67^{b}	7.5 ± 0^{b}	3.75 ± 0.25^{a}	10 ± 0.5^{c}	15 ± 0.67^{d}	17.5 ± 0.3^{e}

Data presented are mean ± standard deviation of three replications. Means with different superscript letters are different by Tukey's posthoc test (p<0.05).

Conclusion

The study of nanoparticle antibacterial properties holds immense promise for both human health and industrial applications. Nanoparticles, due to their unique physicochemical properties, offer versatile solutions for combating bacterial infections and improving hygiene standards. In the realm of human health, nanoparticle-based antibacterial agents have the potential to revolutionize medical treatments. Nanoparticles can be incorporated into wound dressings, surgical implants and medical devices to prevent infections and promote healing. Moreover, nanoparticle-based antimicrobial coatings can be applied to surfaces in healthcare facilities to reduce the transmission of infectious agents and minimize the risk of healthcare-associated infections. Additionally, nanoparticle-based drug delivery systems can enhance the efficacy of antibiotics and antimicrobial agents, enabling targeted delivery and controlled release of therapeutic compounds. From an industrial perspective, the use of nanoparticle antibacterial agents offers numerous benefits across various sectors. In the pharmaceutical industry, nanoparticle-based formulations can be developed for use in topical creams, ointments and oral medications to treat bacterial infections. In the food and beverage industry, nanoparticles can be incorporated into packaging materials to inhibit microbial growth and extend the shelf life of perishable products. Furthermore, in the agriculture sector, nanoparticle-based pesticides and fertilizers can help prevent crop diseases and improve agricultural productivity. Overall, the study of nanoparticle antibacterial properties holds great potential for addressing public health challenges and driving innovation across industries. Further studies are warranted for analysis of the antibacterial potential of the synthesized nanoparticles in an *in vivo* scenario. By harnessing the unique properties of nanoparticles and exploring their diverse applications, researchers and industries can work towards developing effective antibacterial solutions that benefit both human health and industrial processes.

Acknowledgements

The infrastructural financial support under the CURIE programme from the WISE-KIRAN division of the Department of Science and Technology, New Delhi, India to IIS (Deemed to be University), Jaipur, India (File No. DST/CURIE-02/2023/IISU) is gratefully acknowledged. We also acknowledge support from IIS (Deemed to be University), Jaipur, for providing facilities for conducting the above work.

Authors' contributions

RB and LG conceived and designed the experiments. DN performed the experiments. NK and RB performed the analysis of the data. All authors contributed in writing the manuscript.

Compliance with ethical standards

Conflict of interest: Authors do not have any conflict of interests to declare.

Ethical issues: None.

References

1. Velusamy P, Kumar GV, Jeyanthi V, Das J, Pachaiappan R. Bio-inspired green nanoparticles: synthesis, mechanism and antibacterial application. Toxicological Research. 2016;32:95-102. https://doi.org/10.5487/TR.2016.32.2.095
2. Bundschuh M, Filser J, Lüderwald S, McKee MS, Metreveli G, Schaumann GE, et al. Nanoparticles in the environment: where do we come from, where do we go to? Environ Sci Eur. 2018;30:1-17.https://doi.org/10.1186/s12302-018-0132-6
3. Chandra H, Kumari P, Bontempi E, Yadav S. Medicinal plants: Treasure trove for green synthesis of metallic nanoparticles and their biomedical applications. BiocatalAgricBiotechnol. 2020;24:101518.https://doi.org/10.1016/j.bcab.2020.101518
4. Ahmed S, Ahmad M, Swami BL, Ikram S. Green synthesis of silver nanoparticles using *Azadirachta indica* aqueous leaf extract. Journal of Radiation Research and Applied Sciences. 2016;9:1-7.https://doi.org/10.1016/j.jrras.2015.06.006.
5. Kumari P, Panda PK, Jha E, Kumari K, Nisha K, Mallick MA, Verma SK. Mechanistic insight to ROS and apoptosis regulated cytotoxicity inferred by green synthesized CuO nanoparticles from *Calotropis gigantea* to embryonic zebrafish. Sci Rep. 2017;7:16284. https://doi.org/10.1038/s41598-017-16581-1
6. Khani R, Roostaei B, Bagherzade G, Moudi M. Green synthesis of copper nanoparticles by fruit extract of *Ziziphus spina-christi* (L.) Wild: Application for adsorption of triphenylmethane dye and antibacterial assay. J Mol Liq. 2018;255:541-49. https://doi.org/10.1016/j.molliq.2018.02.010.
7. Sadiq H, Sher F, Sehar S, Lima EC, Zhang S, Iqbal HMN, et al. Green synthesis of ZnO nanoparticles from *Syzygium cumini* leaves extract with robust photocatalysis applications. J Mol Liq. 2021;335:116567. https://doi.org/10.1016/j.molliq.2021.116567
8. Maroušek J, Minofar B, Marouškova A, Strunecký O, Gavurová B. Environmental and economic advantages of production and application of digestate biochar. Environmental Technology and Innovation. 2023;30:103109. https://doi.org/10.1016/j.eti.2023.103109.
9. Kwon G, Bhatnagar A, Wang H, Kwon EE, Song H. A review of recent advancements in utilization of biomass and industrial wastes into engineered biochar. Journal of Hazardous Materials. 2020;400:123242. https://doi.org/10.1016/j.jhazmat.2020.123242.
10. Aswathi VP, Meera S, Maria CGA, Nidhin M. Green synthesis of nanoparticles from biodegradable waste extracts and their applications: a critical review. Nanotechnol Environ Eng. 2022;24:1-21. https://doi.org/10.1007/s41204-022-00276-8.
11. Md. Zobair Al Mahmud. A concise review of nanoparticles utilized energy storage and conservation. Journal of Nanomaterials. 2023;Volume 2023:5432099. https://doi.org/10.1155/2023/5432099.
12. Maroušek J. Review: Nanoparticles can change (bio) hydrogen competitiveness. Fuel. 2022;328:125318. https://doi.org/10.1016/j.fuel.2022.125318
13. Shah M, Fawcett D, Sharma S, Tripathy SK, Poinern GEJ. Green synthesis of metallic nanoparticles via biological entities. Materials. 2015;8:7278-308. https://doi.org/10.3390/ma8115377

14. Parida UK, Das S, Jena PK, Rout N, Bindhani BK. Plant mediated green synthesis of metallic nanoparticles: Challenges and opportunities. Fabrication and self-assembly of nanobiomaterials. William Andrew Publishing. 2016;149-77. https://doi.org/10.1016/B978-0-323-41533-0.00006-4

15. Benelli G, Lukehart CM. Applications of green-synthesized nanoparticles in pharmacology, parasitology and entomology. J Clust.Sci.2017;28:1-2. https://doi.org/10.1007/s10876-017-1165-5

16. Jagtap UB, Bapat VA. Green synthesis of silver nanoparticles using *Artocarpus heterophyllus* Lam. seed extract and its antibacterial activity. Ind Crops Prod. 2013;46:132-37. https://doi.org/10.1016/j.indcrop.2013.01.019

17. Ali K, Ahmed B, Dwivedi S, Saquib Q, Al-Khedhairy AA, Musarrat J. Microwave accelerated green synthesis of stable silver nanoparticles with *Eucalyptus globulus* leaf extract and their antibacterial and antibiofilm activity on clinical isolates. PLoS ONE. 2015;10:e0131178. https://doi.org/10.1371/journal.pone.0131178

18. Jha D. Multifunctional biosynthesized silver nanoparticles exhibiting excellent antimicrobial potential against multi-drug resistant microbes along with remarkable anti-cancerous properties. Mater Sci Eng. 2017;80:659-69. https://doi.org/10.1016/j.msec.2017.07.011.

19. Zhan G, Huang J, Lin L, Lin W, Emmanuel K, Li Q. Synthesis of gold nanoparticles by *Cacumen Platycladi* leaf extract and its simulated solution: toward the plant-mediated biosynthetic mechanism. J Nanopart Res. 2011;13:4957-68. https://doi.org/10.1007/s11051-011-0476-y

20. Akhtar MS, Panwar J, Yun YS. Biogenic synthesis of metallic nanoparticles by plant extracts. ACS Sustain Chem Eng. 2013;1:591-602. https://doi.org/10.1021/sc300118u

21. Kuppusamy P, Yusoff MM, Maniam GP, Govindan N. Biosynthesis of metallic nanoparticles using plant derivatives and their new avenues in pharmacological applications–An updated report. Saudi Pharm J. 2016;24:473-84. https://doi.org/10.1016/j.jsps.2014.11.013

22. Mystrioti C, Xanthopoulou TD, Tsakiridis P, Papassiopi N, Xenidis A. Comparative evaluation of five plant extracts and juices for nanoiron synthesis and application for hexavalent chromium reduction. Sci Total Environ. 2016;539:105-13. https://doi.org/10.1016/j.scitotenv.2015.08.091

23. Shankar SS, Rai A, Ankamwar B, Singh A, Ahmad A, Sastry M. Biological synthesis of triangular gold nanoprisms. Nat Mater. 2004;3:482-88. https://doi.org/10.1038/nmat1152

24. Sathishkumar M, Sneha K, Won SW, Cho CW, Kim S, Yun YS. *Cinnamon zeylanicum* bark extract and powder mediated green synthesis of nano-crystalline silver particles and its bactericidal activity. Colloids Surf B. 2009;73:332-38. https://doi.org/10.1016/j.colsurfb.2009.06.005

25. Jacob SJP, Mohammed H, Murali K, Kamarudeen M. Synthesis of silver nanorods using *Coscinium fenestratum* extracts and its cytotoxic activity against Hep-2 cell line. Colloids Surf B. 2012;98:7-11. https://doi.org/10.1016/j.colsurfb.2012.03.031

26. Kumar B, Smita K, Cumbal L, Debut A. Green synthesis of silver nanoparticles using Andean blackberry fruit extract. Saudi J Biol Sci. 2017;24:45-50. https://doi.org/10.1016/j.sjbs.2015.09.006

27. Laily N, Kusumaningtyas RW, Sukarti I, Rini MRDK. The potency of guava *Psidium guajava* (L.) leaves as a functional immunostimulatory ingredient. Procedia Chemistry. 2015;14:301-07.https://doi.org/10.1016/j.proche.2015.03.042

28. Wang L, Wu Y, Xie J, Wu S, Wu Z. Characterization, antioxidant and antimicrobial activities of green synthesized silver nanoparticles from *Psidium guajava* L. leaf aqueous extracts. Mater Sci Eng C. 2018;86:1-8. https://doi.org/10.1016/j.msec.2018.01.003

29. Le NTT, Trinh BT, Nguyen DH, Tran LD, Luu CH, Hoang Thi TT. The physicochemical and antifungal properties of eco-friendly silver nanoparticles synthesized by *Psidium guajava* leaf extract in the comparison with *Tamarindus indica*. J Clust Sci. 2021;32:601-11. https://doi.org/10.1007/s10876-020-01823-6

30. Yugandhar P, Vasavi T, Uma Maheswari Devi P, Savithramma N. Bioinspired green synthesis of copper oxide nanoparticles from *Syzygiumal ternifolium* (Wt.) Walp: characterization and evaluation of its synergistic antimicrobial and anticancer activity. Appl Nanosci. 2017;7:417-27. https://doi.org/10.1007/s13204-017-0584-9

31. Sathiyavimal S, Vasantharaj S, Veeramani V, Saravanan M, Rajalakshmi G, Kaliannan T, et. al. Green chemistry route of biosynthesized copper oxide nanoparticles using *Psidium guajava* leaf extract and their antibacterial activity and effective removal of industrial dyes. J Environ Chem Eng. 2021;9:105033. https://doi.org/10.1016/j.jece.2021.105033

32. Ramya V, Kalaiselvi V, Kannan SK, Shkir M, Ghramh HA, Ahmad Z, et. al. Facile synthesis and characterization of zinc oxide nanoparticles using psidium guajava leaf extract and their antibacterial applications. Arab J Sci Eng. 2022;47:909-18. https://doi.org/10.1007/s13369-021-05717-1

33. Sen A, Batra A. Evaluation of antimicrobial activity of different solvent extracts of medicinal plant: *Melia azedarach* L. Int J Curr Pharm Res. 2012;4:67-73.

34. Li S, Shen Y, Xie A, Yu X, Qiu L, Zhang L, Zhang Q. Green synthesis of silver nanoparticles using *Capsicum annuum* L. extract. Green Chem. 2007;9:852-58. https://doi.org/10.1039/B615357G

35. Vijayakumar G, Kesavan H, Kannan A, Arulanandam D, Kim JH, Kim KJ, et. al. Phytosynthesis of copper nanoparticles using extracts of spices and their antibacterial properties. Processes. 2021;9:1341. https://doi.org/10.3390/pr9081341

36. Padil VVT, Černík M. Green synthesis of copper oxide nanoparticles using gum karaya as a biotemplate and their antibacterial application. Int J Nanomed. 2013;8:889-98. https://doi.org/10.2147/IJN.S40599

37. Esmaile F, Koohestani H, Abdollah-Pour H. Characterization and antibacterial activity of silver nanoparticles green synthesized using *Ziziphora clinopodioides* extract. Environ Nanotechnol Monit Manag. 2020;14:100303. https://doi.org/10.1016/j.enmm.2020.100303

38. Sorbiun M, ShayeganMehr E, Ramazani A, TaghaviFardood S. Green synthesis of zinc oxide and copper oxide nanoparticles using aqueous extract of oak fruit hull (jaft) and comparing their photocatalytic degradation of basic violet 3. Int J Environ Res. 2018;12:29-37. https://doi.org/10.1007/s41742-018-0064-4

39. Jayachandran A, Aswathy TR, Nair AS. Green synthesis and characterization of zinc oxide nanoparticles using *Cayratia pedata* leaf extract. Biochem Biophys Rep. 2021;26:100995. https://doi.org/10.1016/j.bbrep.2021.100995